energies

MDPI

Article

Development of a Dual-Chamber Pyrolizer for Biochar Production from Agricultural Waste in Sri Lanka

W. A. M. A. N. Illankoon [1,*], Chiara Milanese [2], Anurudda Karunarathna Karunarathna [3], A. M. Y. W. Alahakoon [3], Puhulwella G. Rathnasiri [4], Maria Medina-Llamas [2,5], Maria Cristina Collivignarelli [6] and Sabrina Sorlini [1,*]

1 Department of Civil, Environmental, Architectural Engineering, and Mathematics (DICATAM), University of Brescia, Via Branze 43, 25123 Brescia, Italy
2 Department of Chemistry & Center for Colloid and Surface Science, University of Pavia, Viale Taramelli 16, 27100 Pavia, Italy
3 Department of Agricultural Engineering, Faculty of Agriculture, University of Peradeniya, Peradeniya 20400, Sri Lanka
4 Department of Chemical and Process Engineering, University of Moratuwa, Bandaranayake Mawatha, Moratuwa 10400, Sri Lanka
5 Unidad Académica Preparatoria, Plantel II, Universidad Autónoma de Zacatecas, Zacatecas 98068, Mexico
6 Department of Civil Engineering and Architecture, University of Pavia, Via Ferrata 3, 27100 Pavia, Italy
* Correspondence: a.wijepalaabeysi@unibs.it (W.A.M.A.N.I.); sabrina.sorlini@unibs.it (S.S.)

Abstract: This study investigates the design and development of a pyrolysis reactor for batch-type biochar production from rice husks. The main objective is to develop an appropriate technology to regulate pyrolysis temperature and biomass residence time that can be easily operated under field and household conditions with minimal operational and technical requirements. The designed novel dual-chamber reactor comprises two concentrical metal cylinders and a syngas circulation system. The outer cylinder is for energy generation and the inner one is for pyrolysis. Temperature profiles, energy exchanges, syngas production, and the physicochemical characteristics of biochar were obtained to determine the performance of the reactor. Different trials were carried out to obtain different pyrolysis temperatures under constant amounts of feedstock and fuel. The temperature was monitored continuously at three predetermined reactor heights, the temperature profile varied from 380 °C to 1000 °C. The biochar yield was 49% with an average production rate of 1.8 ± 0.2 kg h^{-1}. The reactor consumed 11 ± 0.1 kg of rice husk as feedstock and 6 ± 1 kg h^{-1} of wood as fuel. The gaseous products from the pyrolysis were CH_4, CO_2, H_2, CO, and C_nH_m, which contributed 23.3 ± 2.3 MJ m^{-3} of energy as fuel for the pyrolysis process. The specific surface area of the biochar was 182 m^2 g^{-1}. The achieved operational capacity and thermal efficiency of the reactor show biochar production is a suitable option to convert discarded biomass into a value-added product that can potentially be used in several environmental applications.

Keywords: rice husk; pyrolysis reactor; pyrolysis; energy; agricultural residues; biochar; Sri Lanka; decarbonization; green technologies

Citation: Illankoon, W.A.M.A.N.; Milanese, C.; Karunarathna, A.K.; Alahakoon, A.M.Y.W.; Rathnasiri, P.G.; Medina-Llamas, M.; Collivignarelli, M.C.; Sorlini, S. Development of a Dual-Chamber Pyrolizer for Biochar Production from Agricultural Waste in Sri Lanka. *Energies* **2023**, *16*, 1819. https://doi.org/10.3390/en16041819

Academic Editors: Marcin Sajdak, Roksana Muzyka and Grzegorz Gałko

Received: 20 January 2023
Revised: 3 February 2023
Accepted: 9 February 2023
Published: 11 February 2023

1. Introduction

Biochar production methods are widely used to enhance soil quality and address environmental problems [1–3]. Due to rapid urbanization and industrialization, large quantities of pollutants are released into freshwater bodies. When the concentration of these pollutants in drinking water or wastewater reaches a certain level, the water is no longer safe to drink or use for human purposes. At this stage, there is a need for an effective treatment method that addresses these environmental problems, that can be inexpensive and suitable for large-scale applications. In this case, biochar adsorption technology is considered a suitable option. Many scholars have found it to be an ideal

method for removing various types of pollutants from water [4–10]. Biochar is a low-density carbon substance generated by the thermal degradation of biomass with or without oxygen [11–13], it has multiple mineral components and is distinguished by its porous structure, high specific surface area, and many surfaces functional groups [14,15]. Due to its physicochemical characteristics, biochar has recently attracted great attention for a wide range of applications (Figure 1) [16–19].

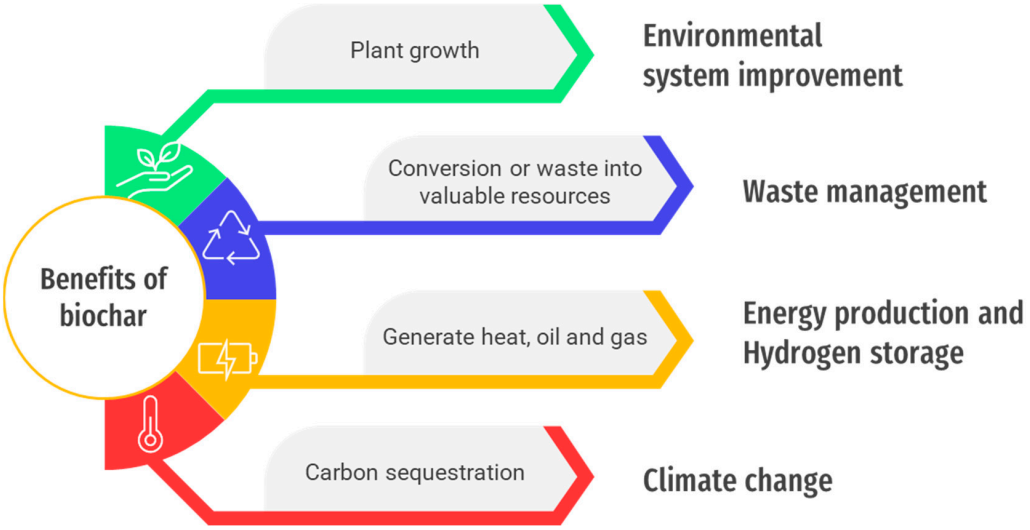

Figure 1. Utilization of biochar in various environmental sectors [16–19].

Biochar System for Global Smallholder Agriculture

A significant proportion of farms in the world are smallholding [20,21]. Small farms comprise the vast majority (562 million) of the world's agricultural activities. However, about 25% of the entire agricultural land is occupied by farms of typical size (average size is 1260 M ha) [20,22,23]. It is estimated that 2.6 billion individuals working on small farms provide food to meet more than 70% of the global demand [24]. To lessen reliance on commercial fertilizers and reduce food production costs, biochar produced from agricultural waste from smallholder farms might be a sustainable solution.

Large amounts of agricultural leftovers such as cereal straw and rice husk, bagasse, and tree limbs might be converted into resources rather than waste. Currently, many stakeholders engage in agricultural sectors practice the open burning of agricultural waste, leading to air pollution [25]. Reports on sustainable biochar production in South India found that it could increase the systemic resilience of farming-based communities in Karnataka; small-scale biochar systems might be beneficial for accomplishing this goal [26]. Therefore, we expect the results of this research will provide a suitable solution for agricultural waste, without capitalizing on its potential uses, as mentioned in Figure 1. Small-scale biochar production is claimed to be more cost-effective than industrial production [27–29]. Several types of small-scale batch-type and industrial scale continuous type biochar production technologies have been reported worldwide, such as earth pit kiln, earth mound kiln, Casamance earth mound kiln, metal kiln, brick kiln, Reichert kiln, retort kiln, multiple hearth reactors, screw type pyrolizers, paddle drum type reactors, and the carbonex kiln [29–32]. The usage of each of these reactors is accompanied by its own set of benefits and drawbacks, which are mentioned in Table 1. Although there are several initiatives to promote biochar production worldwide, conventional biochar production techniques at the small scale and industrial production methods must be improved. As a matter of fact, only a few research studies are available that describe the kiln's design with data on biochar's production and quality. The studies outlined that it is important to control the amount of oxygen (O_2) the biomass is exposed to in order to produce enough heat to carry out the process. Therefore, taking into account these aspects is crucial to produce high-quality

biochar. Table 1 shows the challenges associated with pyrolyzing biomass at small and industrial scales.

Table 1. Comparison of various types of reactors for biochar production [29–32].

Production Type	Reactor Type	Advantages	Disadvantages
Small-scale batch-type processes	Earth pits and mounds, brick, concrete and double metal kilns, retorts	Portable, low-cost, and simple technological solution.	Inefficient, low yield, no heat recovery, hence, much of the feedstock is burned up. Pyrolysis gas and vapors are released into the air, polluting the environment. No control of the pyrolysis temperature, homogeneity of the final product. Some methods are unsafe and require high volumes of water to cool down biochar.
Industrial-scale continuous processes	Retort, multiple hearth reactors, screw type pyrolizers	Higher yields; feedstock flexibility; heat integration; possible co-generation of char and energy; technology that is easy to use and has been available for a long time; co-generation of char and energy; the unit that can be moved or be stationary (depending on size).	Systems that are more sophisticated and have higher costs than batch operations. There are no useful byproducts.
	Paddle drum type reactors	Feedstock flexibility; proven technology; integrated char and energy generation; available as a portable or fixed system (depending on size); greater yields, heat integration, and potential co-production of char and energy.	Complex system; higher cost than batch processes.

Our investigation is focused on rice husk, the most common agricultural waste from the rice sector in Sri Lanka and other Southeast Asian nations. Its production is increasing with growing paddy production patterns [25,33,34]. However, in many developing countries, direct burning is the most common approach to managing this agricultural waste, but it is not an environmentally friendly solution [25,33,35]. Although, during the parboiling process, the rice husk produced in the rice mills is used to generate steam [25]. Producing biochar is a sustainable alternative to direct burning, as described in Figure 1. Therefore, in this work, a dual-chamber pyrolizer was designed with the intention of promoting high-quality biochar production in small and medium-scale paddy farmers and householders due to its appropriateness as a technology that requires minimal specialized operations and it is easy to use. This research uses rice husk as a useful resource to produce biochar without disrupting the conventional parboiling process. This work analyzes the effect of using the produced syngas as an additional heat source during pyrolysis. The productivity and efficiency of the dual-chamber biochar furnace is evaluated by varying the O_2 flow. In addition, evaluate the physicochemical characteristics of the produced biochar under different O_2 inputs. Thereby, this study is designed to test the hypothesis that, "Performance efficiency of a simplified pyrolysis reactor can be improved by controlling the input volumetric air flowrate".

2. Materials and Methods

2.1. The Feedstocks

Rice husk was selected as the feedstock for biochar production, and Gliricidia (*Gliricidia sepium*) wood was chosen as the primary energy source for the pyrolizer. Rice husk was collected from medium-sized rice mills in the north-central province of Sri Lanka, air dried, and suitably stored till its use in the reactor.

2.2. Dual-Chamber Pyrolizer

The introduced dual-chamber pyrolizer is based on the basic principle of indirect heating of biomass with minimum oxygen content. The reactor was introduced as a small-scale and household-level biochar production technique because most of the existing small-scale reactors do not have the ability to control the operational parameters such as temperature and biomass retention time. The novelty of the idea is mainly its ability to control fuel: air ratio and the recirculation of the generated syngas within the reactor to control the pyrolysis temperature and biomass retention time. These modifications enable the production of biochar from different biomass types with different pyrolysis conditions. The dual-chamber biochar reactor was developed using an empty oil barrel as the outer chamber. The reactor consisted of six parts (Figures 2 and 3) and the specifications of each part of the reactor are described in Table 2.

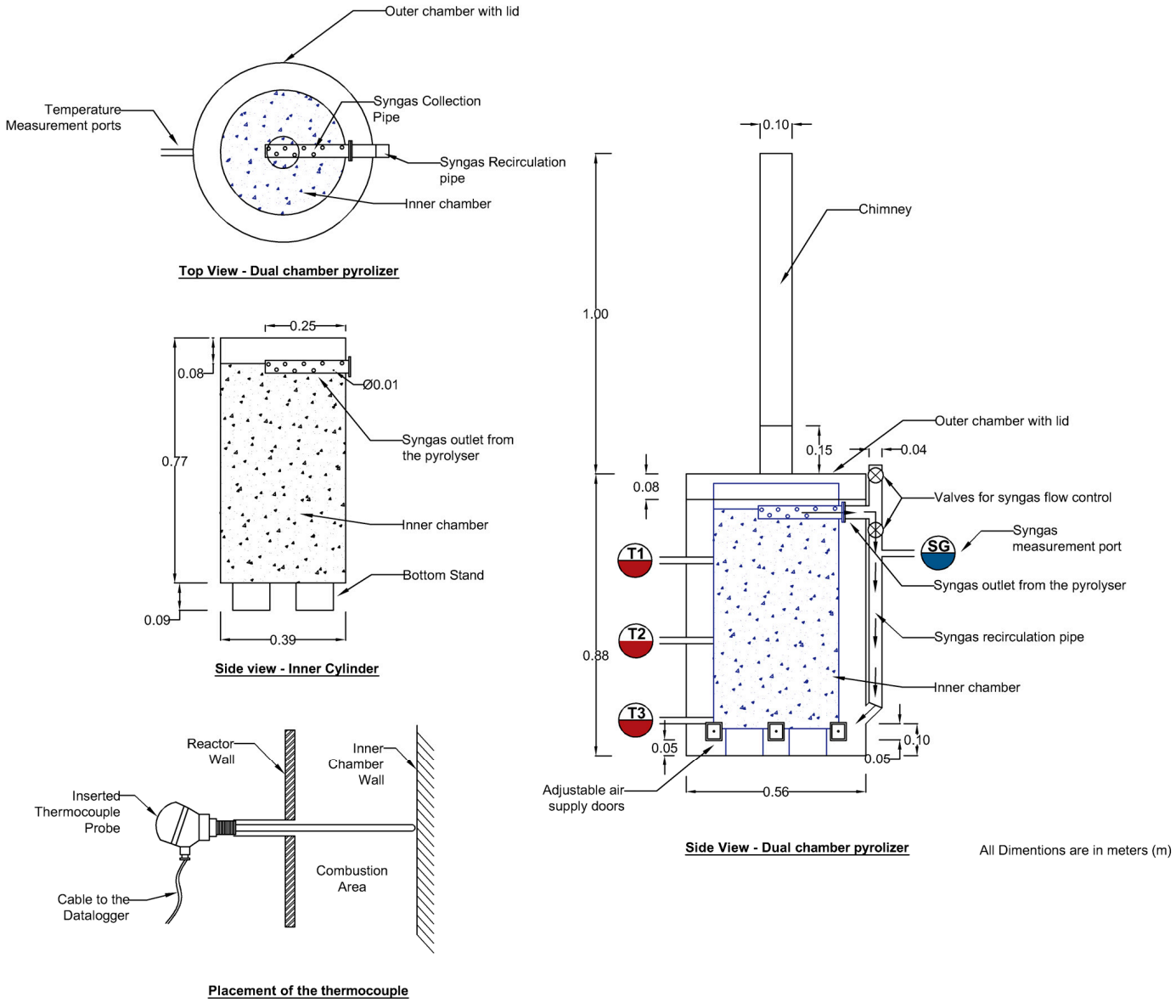

Figure 2. Schemes of the dual-chamber pyrolizer.

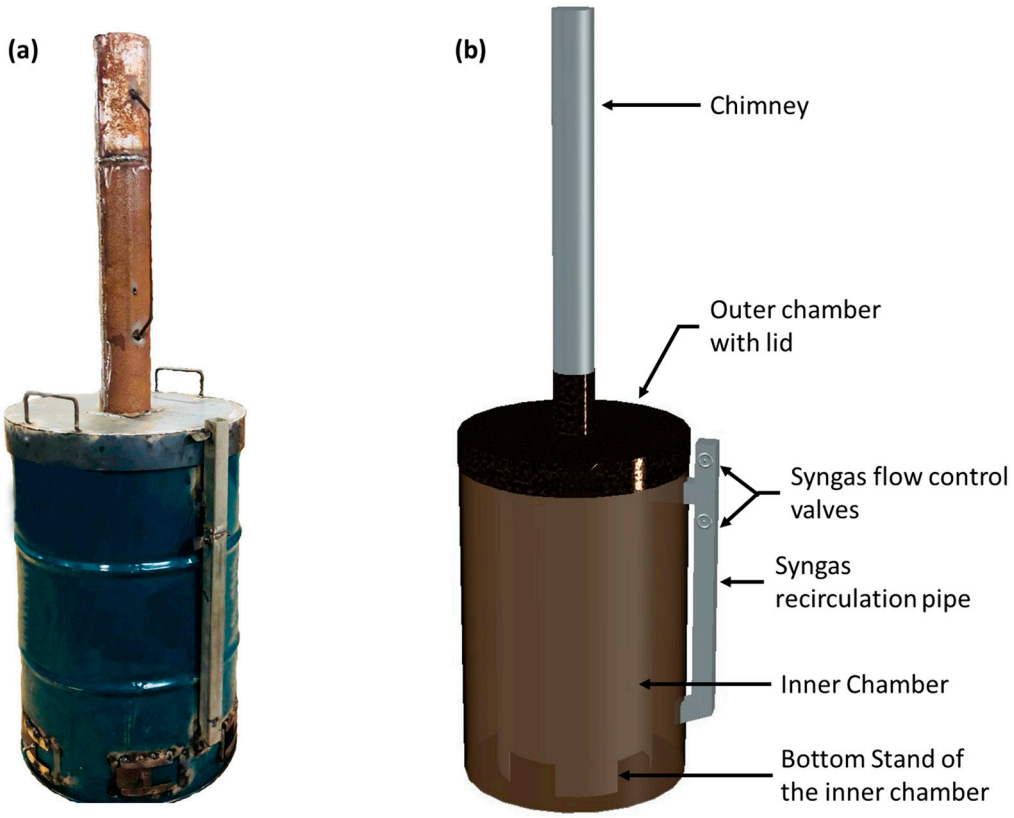

Figure 3. Image of the fabricated dual-chamber reactor: (**a**) actual reactor, (**b**) 3D model of the reactor.

Table 2. Specifications of the dual-chamber reactor.

System Component	Description	Dimensions (Diameter × Height)
Outer chamber	Material—Used oil barrel. Modifications were made in the oil barrel to achieve the design requirements.	0.56 m × 0.88 m
Inner chamber	Material—Gauge 14 (0.016 m) thick steel metal sheet. A 0.01 m high stand was fabricated at the bottom of the cylinder to facilitate a proper heat supply from the bottom of the reactor.	0.39 m × 0.76 m
Lid of the outer chamber	Material—Gauge 14 (0.016 m) thick steel metal sheet. The lid comprised an exhaust gas opening to connect the chimney.	0.56 m × 0.08 m
Lid of the inner chamber	Material—Gauge 14 (0.016 m) thick steel metal sheet. Tightly fixed to minimize oxygen supply.	0.39 m × 0.08 m
Chimney	Material—Gauge 14 (0.016 m) thick steel metal sheet. Fixed to the outer chamber lid to facilitate the updraft of the exhaust gas.	0.10 m × 1.0 m
Syngas circulation pipe	Material—1 mm thick galvanized square tube. Fabricated in two parts for easy dissembling during cleaning, 1 cm holes were drilled in the tube section inside the pyrolizer.	0.032 m × 0.032 m (tube cross section)

Figure 3 shows an image and 3D model of the fabricated dual-chamber reactor. Figure 4 shows the steps to set up the reactor. The inner chamber, with a 39 cm diameter, was designed to store rice husk and produce biochar by using the heat coming from the outer chamber. The bottom of the outer chamber was sealed, and the top was left open. The open top was used to insert the inner chamber into the outer chamber. Wood chips were used to generate heat by combustion. After inserting the inner chamber into the outer chamber, the syngas outlet valve from the inner chamber was connected to the syngas

circulation pump mounted on the surface of the outer chamber (Figure 4a). Subsequently, the rice husk was fed into the inner chamber, which was closed with its lid. At the same time, wood chips were arranged in the outer chamber space between the inner and outer chamber (Figure 4b–d). Six air supply doors were designed on the bottom surface of the outer chamber. Four tests were conducted to analyze the temperature profiles and biochar characteristics. The air supply was controlled by adjusting the air supply doors during each experiment, and the syngas supply was controlled by using syngas flow control valves. Four different tests were performed:

- Trial 1: all air supply doors were fully opened, and syngas was supplied as fuel from the beginning of syngas generation.
- Trial 2: air supply for the combustion was reduced by half by controlling the size of the air supply doors, and syngas was supplied as fuel from the beginning of syngas generation.
- Trial 3: all air supply doors were opened, and the produced syngas was taken out from the reactor.
- Trial 4: all air supply doors were closed, and the produced syngas was taken out from the reactor.

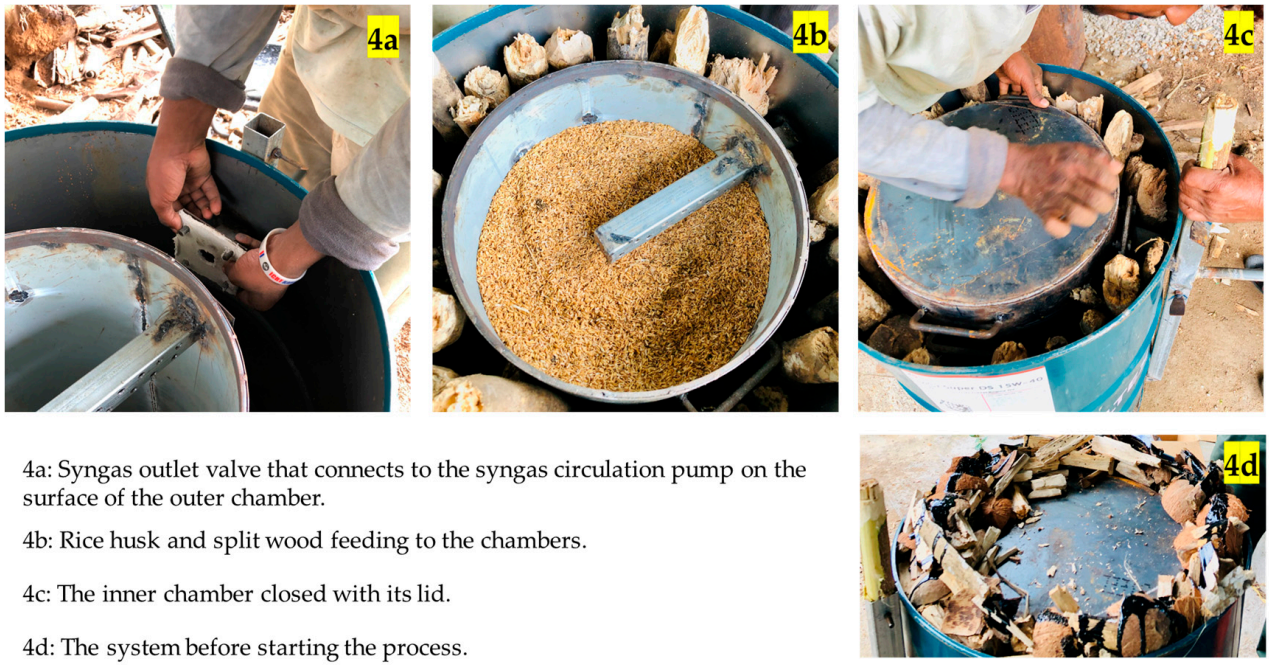

4a: Syngas outlet valve that connects to the syngas circulation pump on the surface of the outer chamber.

4b: Rice husk and split wood feeding to the chambers.

4c: The inner chamber closed with its lid.

4d: The system before starting the process.

Figure 4. Dual-chamber pyrolizer start-up process.

2.3. Performance Evaluation of Dual-Chamber Reactor

The reactor's performance was assessed during each trial of batch operation by varying volumetric air flow rate and the syngas recirculation flow rate was kept constant. The temperature was monitored and mass balances were performed for both wood and rice husk. The reactor's performance was assessed during each batch operation by monitoring its temperature, mass balance, and volumetric flow rate. These findings aided in characterizing the reactor performance and in making comparisons among each trial. In addition, the behavior of the combustion chamber was analyzed by calculating the heat loss that occurred throughout the process. The basic energy balance for the reactor was performed by applying the first law of thermodynamics where energy can be neither created nor destroyed; thus, for any system, the following Equation (1) applies [36]. This helped to find out the theoretical heat loss during the batch operation, and thereby the efficiency of the

reactor. The energy content of each biomass material was calculated using Equation (2) and the energy balance (Equation (1)) was used to calculate the theoretical heat losses:

$$E_{fs} + E_{fuel} = E_{biochar} + E_{sg} + E_{Exh} + E_{Losses} \quad (1)$$

$$Q = C \cdot M \quad (2)$$

where E_{fs} is the energy content of feedstock (MJ), E_{fuel} is the energy content of fuel wood (MJ), $E_{biochar}$ is the energy content of produced biochar (MJ), E_{sg} is the energy content of the produced syngas (MJ), E_{Exh} is the energy content of the exhaust gas produced from the combustion (MJ), and E_{Losses} is the heat losses from the reactor wall (MJ). In Equation (2), Q is the energy content of the biomass material (MJ), C is the heating value of the material (MJ/m^3), and M is the mass of the material (kg).

2.4. Quality of the Produced Biochar

The biochar produced from rice husk in the dual-chamber pyrolizer was analyzed physically, chemically, and proximately. Since the synthesized biochar was intended for use in various environmental applications. ASTM D3172-13, the standard procedure for proximate analysis of coal and coke, was used to describe the biochar recovered using the following Equation (3). The percentage recovery of the biomass was calculated on a wet basis by using Equation (3), where $W_{biochar}$ is the weight of biochar obtained per batch and $W_{feedstock}$ is the weight of wet feedstock biomass used per batch.

$$\%\ \text{Recovery} = \frac{W_{biochar}}{W_{feedstock}} \cdot 100 \quad (3)$$

2.5. Characterization

Analyses were performed on the raw husk and on the pyrolyzed samples by various instrumental techniques. The thermal behavior of the samples was described using thermo-analytical methods. The thermogravimetric curves were acquired by a thermogravimetric analyzer (TGA Q5000, TA Instruments Inc., Lindon, UT, USA) interfaced with a TA5000 data station by heating about 5 mg of powder in a Pt crucible under N_2 flux (50 mL min^{-1}) from 25 °C to 1000 °C at 10 °C/min. Differential scanning calorimetry (DSC) was performed by a Q2000 apparatus (TA Instruments, New Castle, DE, USA) interfaced with a TA5000 data station by heating about 3 mg of powder in an open aluminum crucible from −50 °C to 350 °C and then cooling down to −50 °C (heating and cooling rate = 5 °C min^{-1}) under nitrogen flux (50 mL min^{-1}). Three independent measurements were taken on each sample. The temperature accuracy of the instrument is ±0.1 °C, the precision is ±0.01 °C, and the calorimetric reproducibility is ±0.05%. DSC data were analyzed by the Universal Analysis software by TA Instruments. X-ray diffraction patterns of each sample were obtained (Bruker D2 diffractometer, Ettlingen, Germany) using a zero-background sample holder in the 2θ range 5°–50° with CuKα radiation, step scan of 0.02° and a counting time of 2 s/step at 40 KV and 40 mA. The structural properties of the samples were analyzed at room temperature using the Nicolet FTIR iS10 spectrometer (Nicolet, Madison, WI, USA) equipped with Smart iTR with a diamond plate. The biochar was dried at 45 °C before analysis. Thirty-two scans in the 4000–600 cm^{-1} range at 4 cm^{-1} resolution were coadded. The elemental compositions of the pyrolyzed samples were analyzed by energy dispersive X-ray spectrometry (EDX) using a Zeiss EVO MA10 (Carl Zeiss, Oberkochen, Germany) scanning electron microscope equipped with an Oxford Xmax 50 mm^2 detector following the standard procedure (ASTM E 1508). The tests were carried out at a working distance of 8.5 mm and a voltage of 20 kV for electron generation in an ultra-high vacuum environment.

3. Results and Discussion

3.1. Characteristics of Feedstock

The heating of the reactor walls and system components caused an initial high thermal inertia for the reactor. Therefore, energy had to be supplied at the commencement from the heat source in a quantity larger than required to maintain a constant temperature. Due to this, a small quantity (less than 1 kg) of coconut shells, which is a high-energy biomass source, was added to *Gliricidia* wood as an additional energy source at the pyrolizer's combustion area at the beginning of the process. The energetic and compositional parameters of raw rice husk, *Gliricidia* wood, and coconut are shown in Table 3.

Table 3. Characterization of the feedstocks [34,37–49].

Parameters	Feedstocks		
	Rice Husk	***Gliricidia* Wood**	**Coconut Shells**
Moisture content (%)	7.7 [a]	62.3 [b] [42]	8.14–10.53 [b] [37,39]
Specific gravity (kg/m^3)	140 [a]	670 [b] [42]	1738 [b] [47]
Calorific value (MJ/kg)	12. 85–14.02 [b] [44,49]	19.0–20.5 [b] [42,43,48]	34.1 [b] [40]
Fuelwood value index	-	1255 [b] [42]	-
Lignin content (%)	20–25 [b] [45,46]	26.26–26.8 [b] [41,42]	27 [b] [38]
Volatile matter (%)	67.7 [a]	73.1–82.9 [b] [41,43]	67.7–78.3 [b] [37,39]
Fixed carbon (%)	17.0 [a]	10.3 [b] [43]	17.6–20.96 [b] [37,39]
Ash (%)	15.2 [a]	1.11–1.28 [b] [41,43]	0.74–0.73 [b] [39]

[a] Results from laboratory tests conducted in this work. [b] Results obtained from the literature.

3.2. Mass Balance per Batch

Table 4 shows the input and output data for the reactor operational conditions. For each trial, an approximately constant amount of rice husk (about 11 kg) and wood as fuel was used (about 28 kg). The yield of biochar production varied from 42.37% to 49.28%. However, bio-oil was not extracted throughout the process since it was not intended to be a byproduct. As mentioned above, coconut shell (calorific value 8143 kcal/g) was selected as a high-energy supplementary biomass source; since it has high flammability and heat retention capacity. As the amount of coconut shells (supplied in the form of small pieces) is less than 1 kg for each experiment, it was not considered in the calculations.

Table 4. Mass of reactants and products in the reactor and biochar yield (input and output data).

Trial	Wood		Rice Husk		
	Weight of Wood (kg)	**Weight of Ash Residue (kg)**	**Weight of Rice Husk (kg)**	**Weight of Biochar (kg)**	**Biochar Yield (%)**
1	28.6	0.5	10.8	4.7	43.52
2	28.1	1.3	11	4.96	45.05
3	28.2	1.13	11	4.66	42.37
4	28	1.58	11	5.42	49.28

Figure 5a shows the TGA curve of rice husk, which can be divided into four distinct mass losses. Between 45 °C and 120 °C, adsorbed water (about 5% in mass) is released. Next, a weight loss of 16.8% occurs between 150 °C and 310 °C due to the evaporation of the fixed water content. Carbonaceous components such as lignin and cellulose are destroyed between 310 °C and 400 °C, resulting in a mass loss of 36.30%. Additional elimination of various carbonaceous components leads to the last stage of weight loss (10.52%). The total mass loss at 1000 °C is equal to 68.95%. In the dual-chamber reactor, experiments are performed with a higher mass of rice husk 11 kg, compared to 5 mg in the TGA analysis, the mass loss after each trial is 56.48% (Trial 1), 54.95% (Trial 2), 57.63% (Trial 3), and 50.72% (Trial 4). Figure 5b shows the calorimetric profile of rice husk obtained by DSC. The analysis

shows the presence of the two endothermic events due to adsorbed water release and the first decomposition step starting at around 150 °C is confirmed by the TGA analysis.

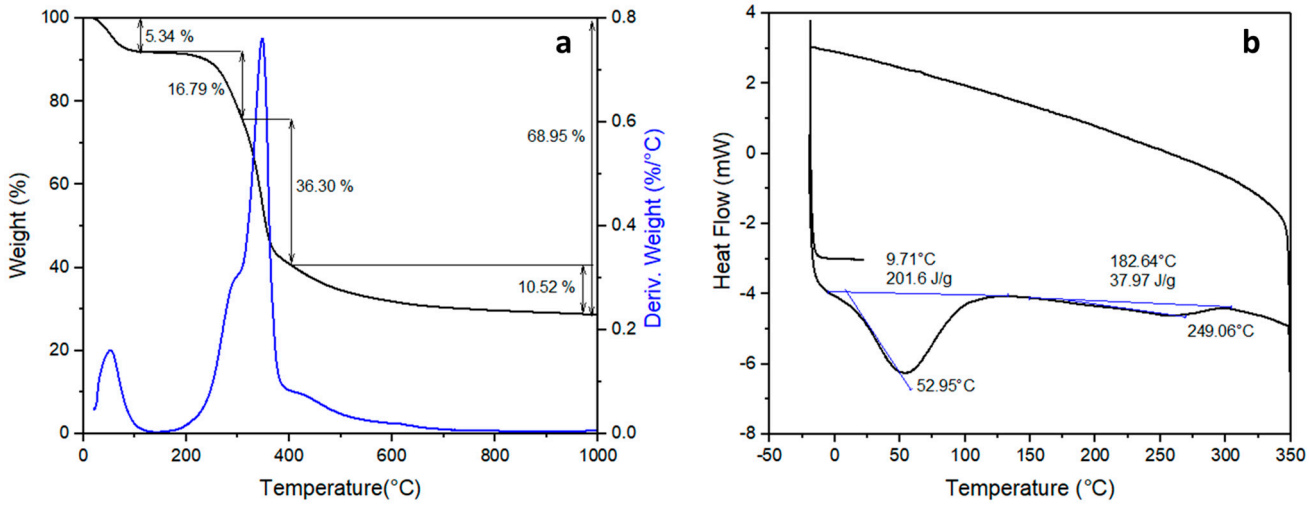

Figure 5. TGA and DTG curves (**a**) and calorimetric profile (**b**) for rice husk (exo up).

3.3. Temperature Profiles

Three temperature measurement ports were fabricated in the outer cylinder wall at a 25 cm distance each. The bottom temperature port was located 10 cm from the bottom edge (Figure 2). During the pyrolysis three continuous temperature profiles of the outer surface of the inner chamber were acquired for each trial, the results are shown in Figure 6. The results show noticeable temperature variations in the reactor's lower zone (T3) compared to the top zones (T1). When the fire front moves down, the reactor employs thermochemical conversion reactions in stratified layers inside the pyrolizer. Reaction completion time changes by varying airflow (O_2) and syngas supply: the times taken to complete the reaction were 176 min (Trial 1), 209 min (Trial 2), 241 min (Trial 3), and 401 min (Trial 4). Trial 1 showed the lowest reaction time; the average temperature varied from 400 °C to 800 °C. According to the data of Trial 4, a long time was needed to complete the reaction when all air supply doors were closed, and syngas was not supplied. Furthermore, the average temperature of T1 and T2 varied between 400 °C and 600 °C. The T3 temperature range was wider than T1 and T2 because the burning charcoals went down to the bottom and induce a temperature rise. It is to underline that the suggested method is more suitable for producing biochar in a lower temperature range but, in this condition, it takes a longer time to complete the reaction, which is a disadvantage. Trials 2 and 3 showed no significant temperature difference or difference in the reaction completion time.

When the rice husk started to become heated, sequential thermochemical reactions started. Rice husk drying takes place initially, in the temperature range of 20–180 °C. The dried rice husk is then subjected to a temperature of 180–250 °C which helps for the torrefaction reactions. Then exothermic pyrolysis takes place at stable temperatures around 250–400 °C. The reactor was designed with the intention of pyrolyzing rice husk at a specific temperature range by varying the airflow (O_2) and syngas supply. However, the temperature profiles fluctuate with the wood-burning rate in the outer chamber. The thermal inertia of the internal pyrolysis cylinder worked as a heat reservoir; thus, temperature changes in the combustion zone did not affect the temperature of the inner pyrolysis cylinder. Therefore, when the temperature in the combustion region decreases, the exothermic reactions may disperse the heat to the biomass, allowing the pyrolysis process to continue [34,50].

Thermochemically, the pyrolysis process is subjected to both endothermic and exothermic reactions, depending on the operating temperature. The exothermic processes of pyrolysis create enough energy to balance out the endothermic reactions [51–53]. Said et al. [54]

performed TGA and DSC tests on rice husk (moisture 9%) and found that the devolatilization process would provide 4.437 kJ/g of energy through fragmentation, reforming, cracking polymerization, and dehydration. This energy might be taken to utilize in pyrolysis' endothermic processes.

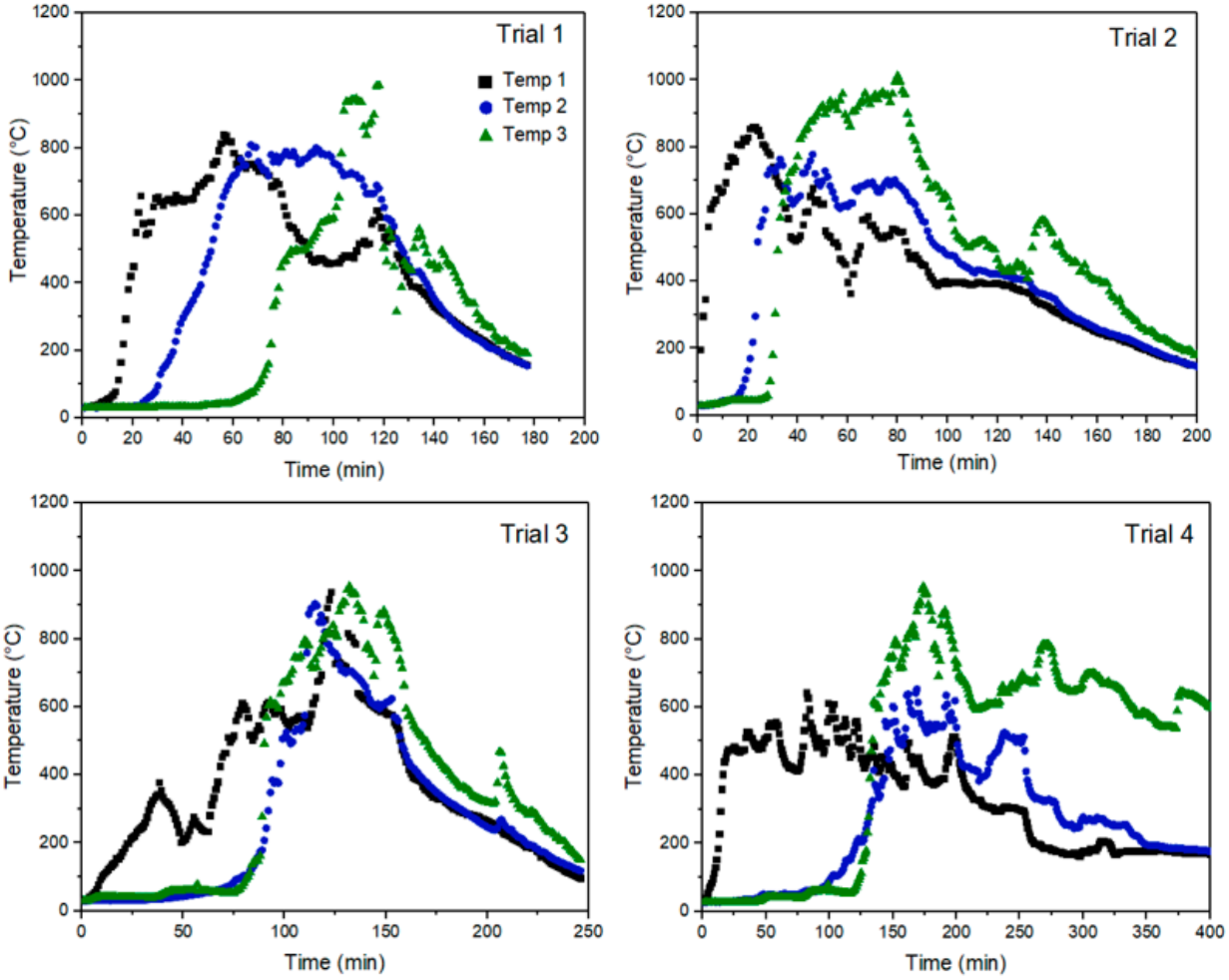

Figure 6. Temperature profiles for the three thermocouples placed in the dual-chamber pyrolizer at different trials.

3.4. Syngas Composition and Energy Value

Figure 7 depicts the chemical composition of the syngas produced by pyrolyzing rice husks and their higher heating values (HHV). Two syngas samples were collected at constant intervals for each trial. The main gaseous products obtained from rice husk pyrolysis are CH_4 (up to 14.29%), CO_2 (up to 33.06%), H_2 (up to 26.38%), CO (up to 25.53%), and C_nH_m (up to 0.94%). From Figure 7, the sequence of the gases generated is essentially consistent across all samples, albeit Trial 2 and Trail 3 exhibit a higher release of syngas and have a maximum HHV.

The catalytic effect of the minerals in pyrolyzed rice husk (ash concentration of about 15.2%) may account for the high hydrogen (H_2) level in the syngas mixture. The literature reports found that the percentage of hydrogen (H_2) released during the pyrolysis of rice husks is proportional to the amount of ash in the husk, suggesting that the ash has a catalytic influence during thermal cracking and, more specifically, in the dehydrogenation process, which in turn increases H_2 generation [55–57]. In addition, oxidized group breakdowns such as decarboxylation and decarbonylating may produce CO and CO_2 [58].

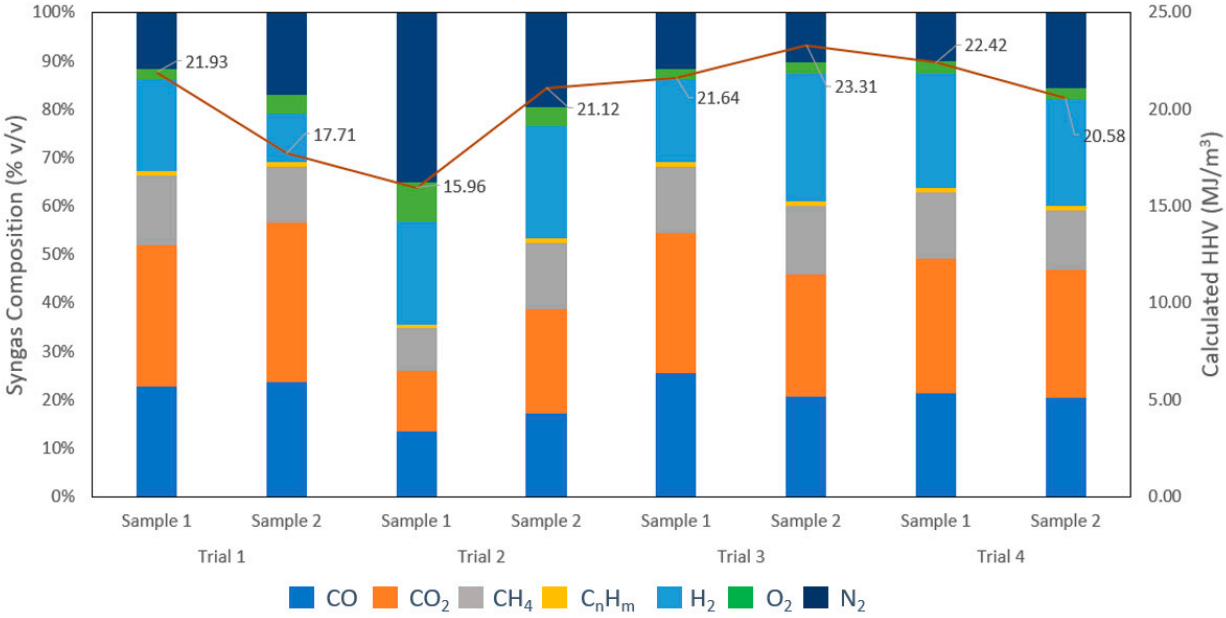

Figure 7. Chemical composition of the syngas and HHV.

Since only H_2, CO, and CH_4 are combustible, the HHV of syngas is the calorific value of these three gases. A mass of 1 kg of biomass is expected to provide 2 m^3 syngas [59–61], hence Equation (4) [59] was used to calculate the HHV of the generated gas combination using the information on fuel HHV and syngas composition:

$$\Delta H\ (2\ m^3\ \text{syngas}) = (HHV_{H2} \times 2\ m^3 \times H_2\%) + (HHV_{CO} \times 2\ m^3 \times CO\%) + (HHV_{CH4} \times 2\ m^3 \times CH_4\%) \quad (4)$$

where HHV_{H2}, HHV_{CO}, and HHV_{CH4} are standard HHV for: H_2 = 12.76 MJ m^{-3}; CO = 12.63 MJ m^{-3}; and CH_4 = 39.76 MJ m^{-3} [62,63]. This investigation achieves a maximum of 23.3 MJ m^{-3} across all pyrolysis settings, suggesting a rich supply of combustible gases. The gas mixture's relatively high heating value could provide supplementary heat for the pyrolysis reactor. The calculated heat capacities of gases fall within the range of those reported in prior research. For example, pyrolysis of solar-dried sewage sludge resulted in gases with an HHV of around 25 MJ m^{-3}, according to reference [64].

3.5. Heat Balance of the Reactor

According to Equation (2), the energy contents of each input and output of the process were calculated and theoretical heat loss for the process was calculated using Equation (1). Table 5 shows the different energy values for the feedstock, fuel, and products yielded from each trial. By using the data, a simple energy balance was conducted. The calculated heat losses are 77.61% (Trial 1), 77.98% (Trial 2), 75.15% (Trial 3), and 74.41% (Trial 4). The results revealed that there is a significant heat loss from the reactor surface due to the absence of an insulation layer. The study suggests the construction of a simple insulation layer such as a brick or clay wall.

3.6. Characteristics of Produced Biochar

3.6.1. Elemental Composition

Biochar's' qualities may be determined from their analytic constituents and H/C and O/C ratios [65,66]. Carbon (C), oxygen (O), silicon (Si), aluminum (Al), potassium (K), and chlorine (Cl) were detected throughout an EDX analysis for each trial (Figure 8). It is to be considered that H is not visible by this technique. As the temperature rises, hydrogen and oxygen are released at a far greater rate than carbon [65]. Based on that, it can be concluded that the waste in Trial 1 has been subjected to a higher temperature than other trials, as it

has lower O content than the other three tests. Thermally-induced CH_4 dehydration is an indication of a shift in biochar recalcitrance [67,68].

Table 5. Energy values for each biomass material in the pyrolysis process for the different trials.

	Trial	Rice Husk	*Gliricidia* Wood	Rice Husk Biochar	Rice Husk Biochar	Exhaust Gas (m^3) *
Mass (kg)	1	10.8	28.6	4.7	30.12	4.88
	2	11.0	28.1	4.96	26.8	4.83
	3	11.0	28.2	4.66	26.97	5.07
	4	11.0	28	5.42	26.42	5.07
Calorific value (MJ/kg)	1	12.85	20.5	12.35	0.27	19.82
	2	12.85	20.5	12.35	0.27	18.53
	3	12.85	20.5	12.35	0.27	22.47
	4	12.85	20.5	12.35	0.27	21.49
Energy content (MJ/batch)	1	138.78	586.3	58.05	8.13	96.72
	2	141.35	576.05	61.26	7.24	89.5
	3	141.35	578.1	57.55	7.28	113.92
	4	141.35	574	66.94	7.13	108.95

* For the exhaust gas, the tabulated values express the volume (m^3) and the calorific value is expressed as MJ m^{-3}.

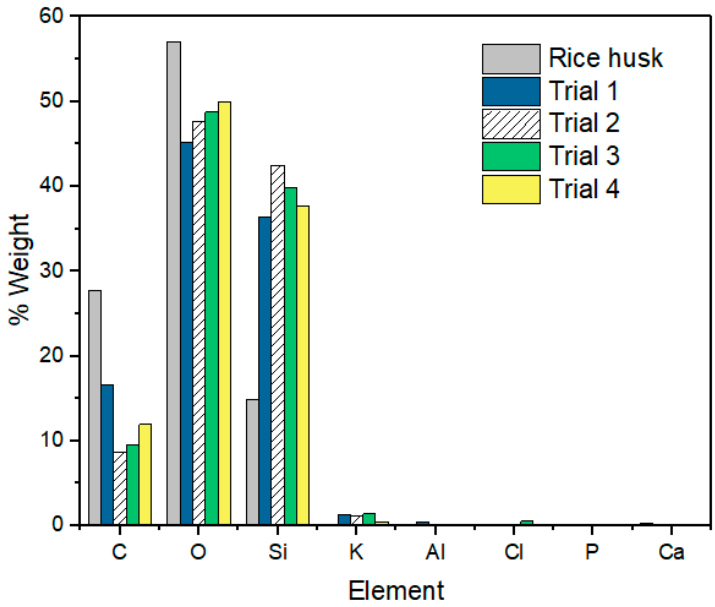

Figure 8. Elemental analysis of the produced biochar.

Furthermore, a biomass material typically contains both labile and recalcitrant O fractions, with the former lost after first heating and preserved in the char of the final product [69]. Charring occurs at high temperatures, leading to dehydration and decarboxylation processes, which reduces the O/C ratios. The O/C ratios in each experiment varied in the following sequence: 5.52 (Trial 2) > 5.15 (Trial 3) > 4.18 (Trial 4) > 2.71 (Trial 1).

To the same extent, a reduced C/O ratio at higher temperatures implies a structural arrangement of the aromatic rings [70], which create highly stable crystal graphite-like structures [71,72]. Since biochar from Trial 2 has a lower C/O ratio (0.18), it is expected to have a stronger graphite-like structure than other samples. Compared to biochar generated from agricultural wastes at lower temperatures, biochar generated from wood at higher temperatures is less biologically labile because it includes a proportionally greater quantity of aromatic-organic matter [73,74]. According to some researchers, the presence of a higher amount of silicon in rice husk biochar creates a dense carbon structure with Si-encapsulated carbon [75]. Figure 8 displays a higher Si concentration in the Trial 2 sample; therefore, Trial 2 biochar may have a dense carbon structure than the other three samples.

3.6.2. Thermal Analysis (TGA and DSC) and Surface Area Results

Thermal analysis is an effective tool for investigating biochar's composition and structure [76,77]. To assess the relative amount of moisture, volatile matter, ash, and fixed carbon in pyrolyzed samples, thermogravimetric analysis was performed. Figure 9 shows the TGA analysis of the biochar obtained in the four trials. At a first glance, it is evident that the TGA profiles of the obtained biochar (Figure 9) are strongly different from the one of the raw rice husk (Figure 5), which is more structured and well-defined, with steps occurring in a sharper way in smaller temperature ranges. First, all the biochar samples followed a similar thermal degradation pattern, with a first step of humidity release (between 4 and 5% for each sample) ending at around 120 °C followed by a huge decomposition step taking place from 150 °C to 1000 °C.

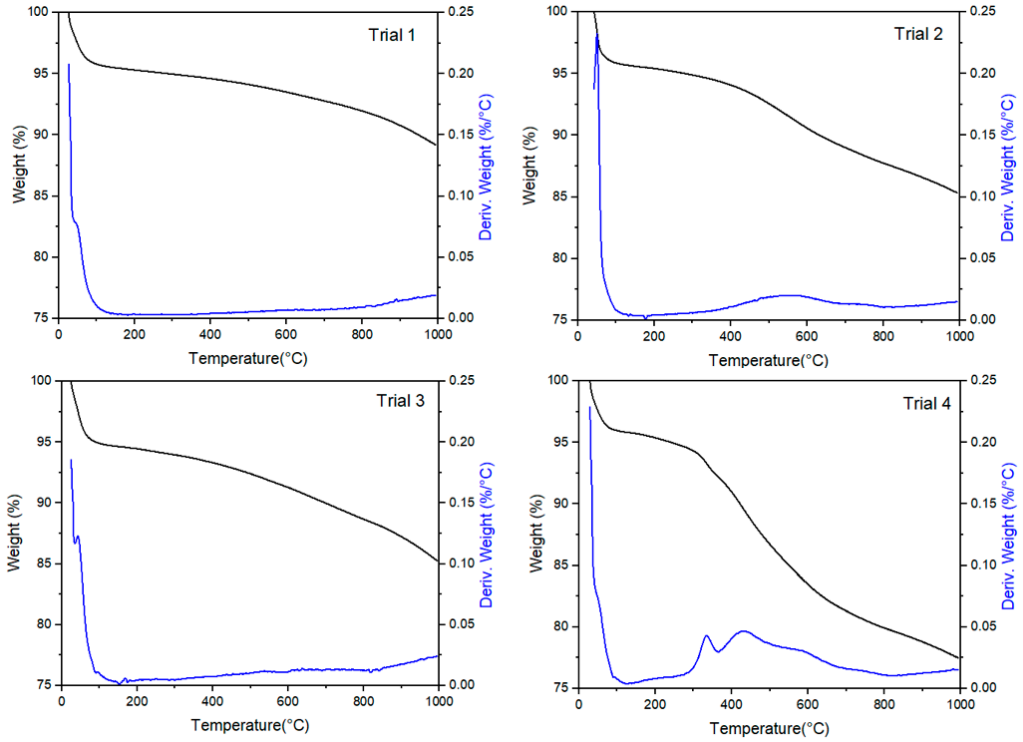

Figure 9. TGA and DTG curves for biochar samples obtained in each trial.

However, some differences can be noticed by observing the shape of this last mass loss step and the evolution of the derivative curve DTG (blue line). In particular, for Trial 1 the degradation rate is slow up to around 600°C, and then gradually increases, probably due to the decomposition of some residual carbonaceous materials such as lignin, cellulose, and hemicellulose [25,78,79]. A similar trend, even if with a higher volatile release is evident for the Trial 3 sample (6% wt. for Trial 1 and 9% wt. for Trial 3). On the contrary, for biochar obtained from Trials 2 and 4, the decomposition is more structured. The DTG curve shows at least two subsequent decomposition processes between 250 °C and 650 °C for Trial 2 and at least three for Trial 4, for which the evolution of processes with different rates is evident also from the TGA curve. From 650 °C to 1000 °C, two other steps of mass release are evident. The mass loss under these steps is 9.6% wt. for Trial 2 and up to 18%, for Trial 4. Therefore, it can be concluded that Trial 4 biochar contains more residual carbonaceous components than the other samples, followed by Trial 2: this points out that for these samples the pyrolysis reaction in the reactor has proceeded to a lower extent.

The release of adsorbed water at a temperature lower than 100 °C and the beginning of a huge and slow decomposition process starting from 150 °C is evident also in the calorimetric profiles (Figure 10), showing a clear endothermic peak ending at around 100 °C and an increasing endothermic variation from the baseline starting at around 150 °C

and more evident in Trial 4 curve. Furthermore, in this case, the profile is different from that of the raw husk (Figure 5b), since the amount of adsorbed water is lower in the pyrolyzed samples. Compare an enthalpy of 200 J/g for the raw material vs. a maximum value of 70 J/g for Trial 2 and 4 and the decomposition steps are slower and less evident (the second peak present in the calorimetric profile of raw husk is a gradual detachment from the baseline in these samples). The lower degradation degree in Trial 4 is evident in its lower surface area as obtained by BET analysis: the surface area of raw rice husk is as low as 2.8 m^2/g and it increases to 182 m^2/g for Trial 1, 141 m^2/g for Trial 2, 168 m^2/g for Trial 3, and 132 m^2/g for Trial 4.

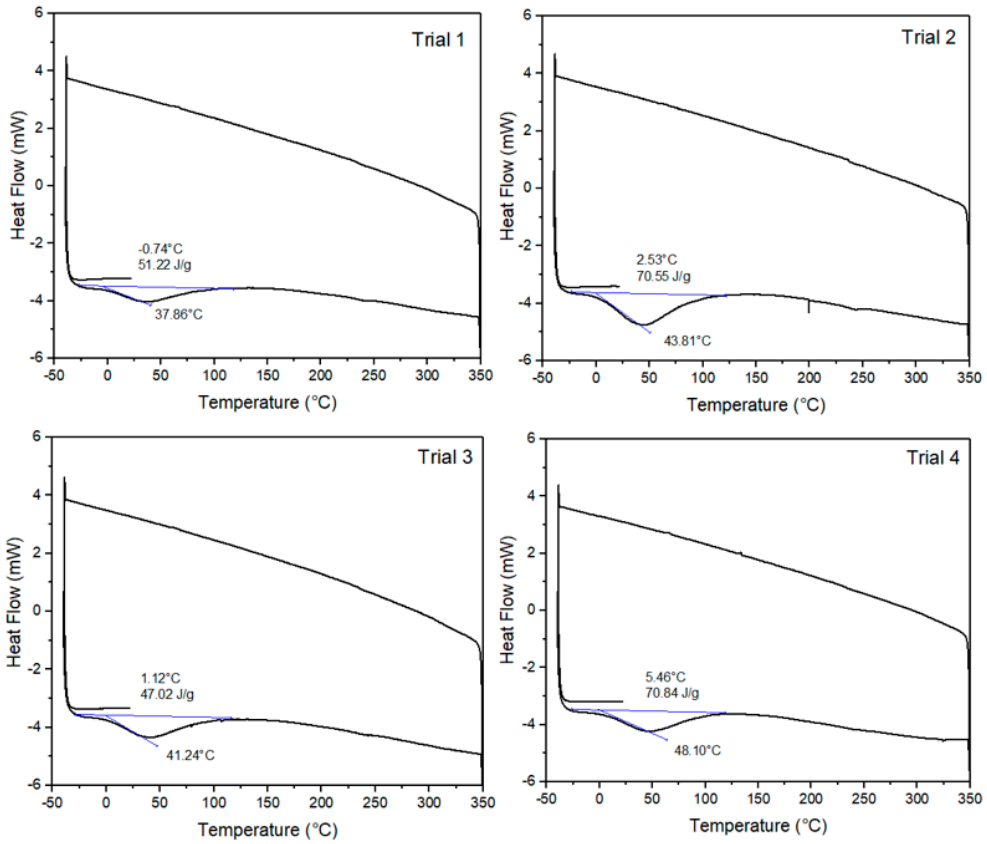

Figure 10. DSC profiles of the pyrolyzed samples (exo up).

3.6.3. Fourier Transform Infrared (FTIR) Spectroscopy

To detect the variation in chemical composition, FT-IR spectroscopy is an effective tool (Figure 11). The C-H (750–900 cm^{-1}), C=C (1380–1450 cm^{-1}) and C-O stretching (1580–1700 cm^{-1}) signals can be seen in all samples, and C=C bonds in the Trial 4 sample caused the most prominent representative peaks for aromatic carbon. Pyrolyzing temperature alters the functional group, as the FTIR spectrum shows a reduction in aliphatic C groups and an increase in aromatic C [80].

According to the literature, the strength of bands such as those corresponding to hydroxyl groups (3200–3400 cm^{-1}) and aromatic groups (1580–1600 and 3050–3000 cm^{-1}) decreases, when the pyrolyzing temperature range is between 700 and 800 °C, while biochar obtained at lower temperatures (300 and 500 °C) include a more significant number of bonds indicating functional groups than those made at 700 °C [81]. Figure 8 and the cited works support the conclusion that all feedstocks were heated to temperatures higher than 700 °C during the biochar synthesis process.

Bands around 800 cm^{-1} and 1040–1100 cm^{-1} were attributed to SiO_2, reflecting the feedstock's composition. These spectral lines were detected in all the trials. Silica, an essential component of phytoliths, prevents carbon in plants from degrading, according to the field of plant physiology [82,83]. Among the many chemical components of rice, silicon

dioxide plays a significant role. The shoulder seen in the FTIR spectrum about 1600 cm^{-1}, which was attributed to aromatic compounds, is still present at temperatures as high as 800 °C during biochar synthesis.

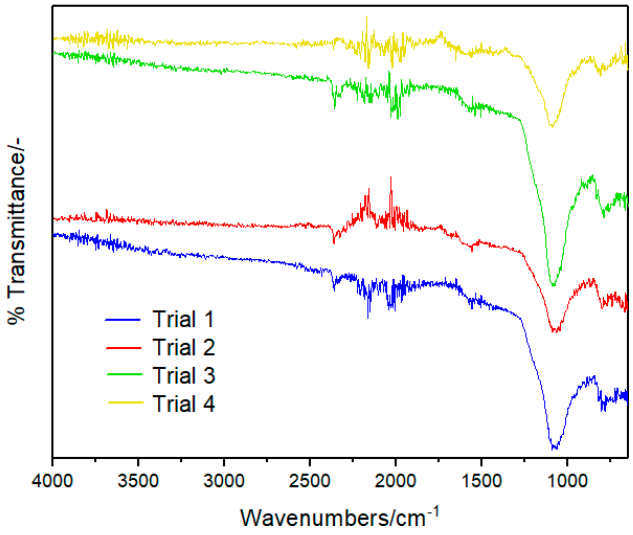

Figure 11. ATR-FTIR spectra of pyrolyzed samples.

3.6.4. XRD

Figure 12 shows the XRD patterns for rice husk (before pyrolysis) and biochar pyrolyzed at the different trial conditions. The XRD patterns of rice husk show the distinctive peaks at 22.4°, 34.1°, and 47.8° that can be assigned to the presence of silica (SiO_2) from rice husk (JCPDS 33-1161). The wide diffraction peaks of the cellulose polymorphs are located around 15°, 17°, and 20°: these wide peaks can be observed only in the rice husk [84]. After pyrolysis, only the peak at 22° due to the C presence is evident and it becomes broader due to the amorphous characteristics of biochar.

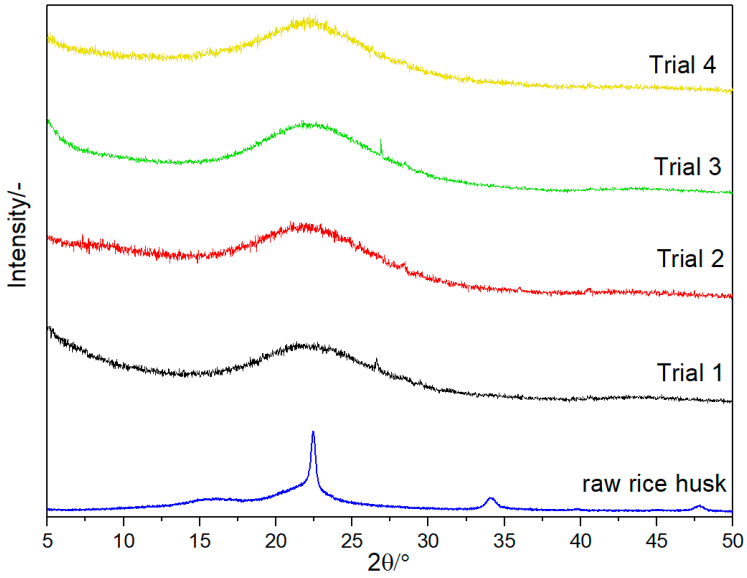

Figure 12. XRD patterns of the rice husk and the pyrolyzed samples.

3.7. Challenges and Future Perspectives

According to the results obtained from four trials, the weight of the biochar produced is nearly the same. However, in Trial 3, the energy content of syngas is higher compared to all other trials. If a farmer uses this syngas to produce heat for cooking or other purposes,

Trial 3 would be beneficial. The main challenge of introducing a new technology is the knowledge dissemination process. There are several circumstances in introducing new technologies to the farmer level with the very low adaptability of farmers to these new technologies. Furthermore, the demand for biomass sources for other purposes such as combustion, animal feed, and incineration also makes it competitive to promote biochar production for agricultural wastes.

The central notion of this investigation is that bio-carbon may be used to create a sustainable, circular bioeconomy, which presents a practical response to the system's dominant administration. Thermochemical technologies employed in biochar synthesis, particularly in rural regions, will aid regional development by allowing small and medium-scale firms to promote industrial symbiosis, boosting farmer income and facilitating waste management in the agricultural sector. Thus, with this method, small-scale production systems may be linked with other systems to create closed system models, where waste from one process can be used as an input for another, resulting in positive social, economic, and ecological consequences in a circular economy. The application of the main product in different environmental applications is also another important aspect to be addressed. Biochar can be used as an adsorbent to remove color and different pollutants in wastewater treatment. In addition, depending on characteristics, heavy metal can also be removed. However, it has to be contained in packed bed columns or other appropriate reactor configurations.

4. Conclusions

The dual-chamber pyrolizer reactor developed in this work was designed to valorize rice industry waste products in rice-growing regions for small-scale applications and batch-type operations. The design specifically has the ability to control the fuel-to-air ratio for combustion by controlling the airflow, as well as it has the ability to utilize produced syngas as needed. With the careful control of airflow and syngas flow, the reactor's capacity to work at temperatures ranging from 400 to 1000 °C was observed. Biochar yielding percentage and quality proved that the dual-chamber reactor can produce biochar from rice husk in the above temperature range at varying biomass residence times (from 200 min up to 400 min). Furthermore, the varying resident times influence the chemical composition of the final product, resulting in a broader range of product quality with varying chemical characteristics. The main gaseous products obtained from rice husk pyrolysis were CH_4 (up to 14.27 $\pm$ 0.08%), CO_2 (up to 33.06 $\pm$ 2.67%), H_2 (up to 26.38 $\pm$ 0.75%), CO (up to 25.53 $\pm$ 0.45%), and C_nH_m (up to 0.94 $\pm$ 0.11%), that also contributed with 23.3 $\pm$ 2.3 MJm^{-3} of energy as a fuel for the pyrolysis process. Recirculating the generated syngas as an energy source for the reactor can minimize the fuel requirement for the process while reducing harmful emissions to the atmosphere. With the above reactor characteristics, small-scale biochar manufacturers will have many advantages from this reactor over other conventional methods, where they can produce biochar at a predetermined temperature and residence time combination. Furthermore, the use of simple and banal fabrication materials such as oil barrels and steel barrels would make it more implementable within the local community. Thereby, the local community can also manipulate the pyrolysis process parameters without in-depth technical knowledge of the pyrolysis process. In the south Asian region, the main use of biochar is for soil application, thus the physiochemical and surface characteristics of produced biochar proved its suitability in soil application. Rice husk biochar produced from this reactor is already being utilized to make a composite fertilizer for various crops, including rice. Additionally, the adaptability of the reactor to different biomass types also requires further investigation. Furthermore, it is necessary to evaluate reactor performance by adding a thermal insulation layer to the outer chamber using locally available materials.

Author Contributions: Conceptualization, W.A.M.A.N.I. and S.S.; methodology, W.A.M.A.N.I., A.M.Y.W.A., A.K.K., P.G.R. and S.S.; software, W.A.M.A.N.I., C.M., A.M.Y.W.A. and M.M.-L.; validation, W.A.M.A.N.I., A.M.Y.W.A., A.K.K. and C.M.; formal analysis, W.A.M.A.N.I.; investigation, W.A.M.A.N.I., A.M.Y.W.A. and A.K.K.; data curation, W.A.M.A.N.I. and A.M.Y.W.A.; writing—original draft preparation, W.A.M.A.N.I.; writing—review and editing, W.A.M.A.N.I., C.M., A.M.Y.W.A., A.K.K., P.G.R., M.M.-L., M.C.C. and S.S.; supervision, C.M., A.K.K., P.G.R., M.C.C. and S.S. All authors have read and agreed to the published version of the manuscript.

Funding: This research received no external funding.

Data Availability Statement: The data presented in this study are available on request from the corresponding author.

Acknowledgments: The authors are grateful to the Department of Agricultural Engineering in the University of Peradeniya, Sri Lanka, and the Postgraduate Institute of Agriculture, University of Peradeniya, Sri Lanka for providing the needful facilities.

Conflicts of Interest: The authors declare no conflict of interest.

References

1. Lehmann, J.; Gaunt, J.; Rondon, M. Bio-Char Sequestration in Terrestrial Ecosystems—A Review. *Mitig. Adapt. Strat. Glob. Chang.* **2006**, *11*, 403–427. [CrossRef]
2. Wu, P.; Ata-Ul-Karim, S.T.; Singh, B.P.; Wang, H.; Wu, T.; Liu, C.; Fang, G.; Zhou, D.; Wang, Y.; Chen, W. A Scientometric Review of Biochar Research in the Past 20 Years (1998–2018). *Biochar* **2019**, *1*, 23–43. [CrossRef]
3. Lehmann, J.; Bossio, D.A.; Kögel-Knabner, I.; Rillig, M.C. The Concept and Future Prospects of Soil Health. *Nat. Rev. Earth Environ.* **2020**, *1*, 544–553. [CrossRef]
4. Xu, Y.; Chen, J.; Chen, R.; Yu, P.; Guo, S.; Wang, X. Adsorption and Reduction of Chromium(VI) from Aqueous Solution Using Polypyrrole/Calcium Rectorite Composite Adsorbent. *Water Res.* **2019**, *160*, 148–157. [CrossRef]
5. Khataee, A.R.; Kasiri, M.B. Photocatalytic Degradation of Organic Dyes in the Presence of Nanostructured Titanium Dioxide: Influence of the Chemical Structure of Dyes. *J. Mol. Catal. A Chem.* **2010**, *328*, 8–26. [CrossRef]
6. Haddad, M.Y.; Alharbi, H.F. Enhancement of Heavy Metal Ion Adsorption Using Electrospun Polyacrylonitrile Nanofibers Loaded with ZnO Nanoparticles. *J. Appl. Polym. Sci.* **2019**, *136*, 47209. [CrossRef]
7. Haddad, M.; Oie, C.; Vo Duy, S.; Sauvé, S.; Barbeau, B. Adsorption of Micropollutants Present in Surface Waters onto Polymeric Resins: Impact of Resin Type and Water Matrix on Performance. *Sci. Total Environ.* **2019**, *660*, 1449–1458. [CrossRef]
8. Mahvi, A.H. Application of Agricultural Fibers in Pollution Removal from Aqueous Solution. *Int. J. Environ. Sci. Technol.* **2008**, *5*, 275–285. [CrossRef]
9. Dehghani, M.H.; Mahvi, A.H.; Rastkari, N.; Saeedi, R.; Nazmara, S.; Iravani, E. Adsorption of Bisphenol A (BPA) from Aqueous Solutions by Carbon Nanotubes: Kinetic and Equilibrium Studies. *Desalination Water Treat.* **2015**, *54*, 84–92. [CrossRef]
10. Roy, H.; Islam, M.S.; Arifin, M.T.; Firoz, S.H. Synthesis, Characterization and Sorption Properties of Biochar, Chitosan and ZnO-Based Binary Composites towards a Cationic Dye. *Sustainability* **2022**, *14*, 14571. [CrossRef]
11. Yuan, Y.; Chesnutt, B.M.; Haggard, W.O.; Bumgardner, J.D. Deacetylation of Chitosan: Material Characterization and in Vitro Evaluation via Albumin Adsorption and Pre-Osteoblastic Cell Cultures. *Materials* **2011**, *4*, 1399–1416. [CrossRef]
12. Regmi, P.; Garcia Moscoso, J.L.; Kumar, S.; Cao, X.; Mao, J.; Schafran, G. Removal of Copper and Cadmium from Aqueous Solution Using Switchgrass Biochar Produced via Hydrothermal Carbonization Process. *J. Environ. Manag.* **2012**, *109*, 61–69. [CrossRef]
13. Beesley, L.; Marmiroli, M. The Immobilisation and Retention of Soluble Arsenic, Cadmium and Zinc by Biochar. *Environ. Pollut.* **2011**, *159*, 474–480. [CrossRef]
14. Tan, K.B.; Vakili, M.; Horri, B.A.; Poh, P.E.; Abdullah, A.Z.; Salamatinia, B. Adsorption of Dyes by Nanomaterials: Recent Developments and Adsorption Mechanisms. *Sep. Purif. Technol.* **2015**, *150*, 229–242. [CrossRef]
15. Maleki, A.; Mahvi, A.H.; Zazouli, M.A.; Izanloo, H.; Barati, A.H. Aqueous Cadmium Removal by Adsorption on Barley Hull and Barley Hull Ash. *Asian J. Chem.* **2011**, *23*, 1373–1376.
16. Palansooriya, K.N.; Ok, Y.S.; Awad, Y.M.; Lee, S.S.; Sung, J.-K.; Koutsospyros, A.; Moon, D.H. Impacts of Biochar Application on Upland Agriculture: A Review. *J. Environ. Manag.* **2019**, *234*, 52–64. [CrossRef] [PubMed]
17. Wani, I.; Ramola, S.; Garg, A.; Kushvaha, V. Critical Review of Biochar Applications in Geoengineering Infrastructure: Moving beyond Agricultural and Environmental Perspectives. *Biomass Convers. Biorefin.* **2021**, 1–29. [CrossRef]
18. Xu, G.; Lv, Y.; Sun, J.; Shao, H.; Wei, L. Recent Advances in Biochar Applications in Agricultural Soils: Benefits and Environmental Implications. *Clean* **2012**, *40*, 1093–1098. [CrossRef]
19. Roy, H.; Prantika, T.R.; Riyad, M.H.; Paul, S.; Islam, M.S. Synthesis, Characterizations, and RSM Analysis of Citrus Macroptera Peel Derived Biochar for Textile Dye Treatment. *S. Afr. J. Chem. Eng.* **2022**, *41*, 129–139. [CrossRef]
20. Yrjälä, K.; Ramakrishnan, M.; Salo, E. Agricultural Waste Streams as Resource in Circular Economy for Biochar Production towards Carbon Neutrality. *Curr. Opin. Environ. Sci. Health* **2022**, *26*, 100339. [CrossRef]

21. Nair, V.D.; Nair, P.K.R.; Dari, B.; Freitas, A.M.; Chatterjee, N.; Pinheiro, F.M. Biochar in the Agroecosystem–Climate-Change–Sustainability Nexus. *Front. Plant Sci.* **2017**, *8*, 02051. [CrossRef] [PubMed]
22. Seeman, T.; Šrédl, K.; Prášilová, M.; Svoboda, R. The Price of Farmland as a Factor in the Sustainable Development of Czech Agriculture (A Case Study). *Sustainability* **2020**, *12*, 5622. [CrossRef]
23. Lowder, S.K.; Skoet, J.; Raney, T. The Number, Size, and Distribution of Farms, Smallholder Farms, and Family Farms Worldwide. *World Dev.* **2016**, *87*, 16–29. [CrossRef]
24. Small Family Farmers Produce a Third of the World's Food. Available online: https://www.fao.org/newsroom/detail/Small-family-farmers-produce-a-third-of-the-world-s-food/en (accessed on 2 January 2023).
25. Illankoon, W.A.M.A.N.; Milanese, C.; Girella, A.; Rathnasiri, P.G.; Sudesh, K.H.M.; Llamas, M.M.; Collivignarelli, M.C.; Sorlini, S. Agricultural Biomass-Based Power Generation Potential in Sri Lanka: A Techno-Economic Analysis. *Energies* **2022**, *15*, 8984. [CrossRef]
26. Müller, S.; Backhaus, N.; Nagabovanalli, P.; Abiven, S. A Social-Ecological System Evaluation to Implement Sustainably a Biochar System in South India. *Agron. Sustain. Dev.* **2019**, *39*, 43. [CrossRef]
27. Clare, A.; Shackley, S.; Joseph, S.; Hammond, J.; Pan, G.; Bloom, A. Competing Uses for China's Straw: The Economic and Carbon Abatement Potential of Biochar. *Bioenergy* **2015**, *7*, 1272–1282. [CrossRef]
28. Leach, M.; Fairhead, J.; Fraser, J. Green Grabs and Biochar: Revaluing African Soils and Farming in the New Carbon Economy. *J. Peasant. Stud.* **2012**, *39*, 285–307. [CrossRef]
29. Schure, J.; Pinta, F.; Cerutti, P.O.; Kasereka-Muvatsi, L. Efficiency of Charcoal Production in Sub-Saharan Africa: Solutions beyond the Kiln. *Bois For. Des. Trop.* **2019**, *340*, 57–70. [CrossRef]
30. Ighalo, J.O.; Eletta, O.A.A.; Adeniyi, A.G. Biomass Carbonisation in Retort Kilns: Process Techniques, Product Quality and Future Perspectives. *Bioresour. Technol. Rep.* **2022**, *17*, 100934. [CrossRef]
31. Mašek, O.; Buss, W.; Roy-Poirier, A.; Lowe, W.; Peters, C.; Brownsort, P.; Mignard, D.; Pritchard, C.; Sohi, S. Consistency of Biochar Properties over Time and Production Scales: A Characterisation of Standard Materials. *J. Anal. Appl. Pyrolysis* **2018**, *132*, 200–210. [CrossRef]
32. Kirch, T.; Medwell, P.R.; Birzer, C.H.; van Eyk, P.J. Small-Scale Autothermal Thermochemical Conversion of Multiple Solid Biomass Feedstock. *Renew Energy* **2020**, *149*, 1261–1270. [CrossRef]
33. Rodrigo, A.S.; Perera, S. Potential and Viability of Rice Husk Based Power Generation in Sri Lanka. *Eng. J. Inst. Eng. Sri Lanka* **2013**, *46*, 9. [CrossRef]
34. Alahakoon, A.M.Y.W.; Karunarathna, A.K.; Dharmakeerthi, R.S.; Silva, F.H.C.A. Design and Development of a Double-Chamber Down Draft (DcDD) Pyrolyzer for Biochar Production from Rice Husk. *J. Biosyst. Eng.* **2022**, *47*, 458–467. [CrossRef]
35. Qian, X.; Xue, J.; Yang, Y.; Lee, S.W. Thermal Properties and Combustion-Related Problems Prediction of Agricultural Crop Residues. *Energies* **2021**, *14*, 4619. [CrossRef]
36. Schoeller, D.A. The Energy Balance Equation: Looking Back and Looking Forward Are Two Very Different Views. *Nutr. Rev.* **2009**, *67*, 249–254. [CrossRef] [PubMed]
37. Hoque, M.M.; Bhattacharya, S.C. Fuel Characteristics of Gasified Coconut Shell in a Fluidized and a Spouted Bed Reactor. *Energy* **2001**, *26*, 101–110. [CrossRef]
38. Jaya Prithika, A.; Sekar, S.K. Mechanical and Fracture Characteristics of Eco-Friendly Concrete Produced Using Coconut Shell, Ground Granulated Blast Furnace Slag and Manufactured Sand. *Constr. Build. Mater.* **2016**, *103*, 1–7. [CrossRef]
39. Li, W.; Yang, K.; Peng, J.; Zhang, L.; Guo, S.; Xia, H. Effects of Carbonization Temperatures on Characteristics of Porosity in Coconut Shell Chars and Activated Carbons Derived from Carbonized Coconut Shell Chars. *Ind. Crops Prod.* **2008**, *28*, 190–198. [CrossRef]
40. Nuriana, W.; Anisa, N. Martana Synthesis Preliminary Studies Durian Peel Bio Briquettes as an Alternative Fuels. *Energy Procedia* **2014**, *47*, 295–302. [CrossRef]
41. Oyelere, A.T.; Oluwadare, A.O. Studies on Physical, Thermal and Chemical Properties of Wood Gliricidia Sepium for Potential Bioenergy Production. *Int. J. Biomass Renew.* **2019**, *8*, 28–38.
42. Mainoo, A.A.; Ulzen-Appiah, F. Growth, Wood Yield and Energy Characteristics of Leucaena Leucocephala, Gliricidia Sepium and Senna Siamea at Age Four Years. *Ghana J. For.* **1996**, *3*, 69–79.
43. Rahayu, S.; Hilyana, S.; Suryani, E.; Nazmi; Sari, H.; Ali, M. Analysis of Wood Pellet Quality from Calliandra Callothyrsus, Gliricida Sepium, and Sawdust as New and Renewable Energy. In *Proceedings of the International Conference on Science and Technology (ICST), Mataram, Indonesia, 16–17 October 2021*; Institute for Research and Research and Community Service: Kota Surakarta, Indonesia, 2021; pp. 110–115.
44. Suryaningsih, S.; Nurhilal, O.; Yuliah, Y.; Mulyana, C. Combustion Quality Analysis of Briquettes from Variety of Agricultural Waste as Source of Alternative Fuels. *IOP Conf. Ser. Earth Environ. Sci.* **2017**, *65*, 012012. [CrossRef]
45. Kumar, P.; Barrett, D.M.; Delwiche, M.J.; Stroeve, P. Methods for Pretreatment of Lignocellulosic Biomass for Efficient Hydrolysis and Biofuel Production. *Ind. Eng. Chem. Res.* **2009**, *48*, 3713–3729. [CrossRef]
46. Gao, Y.; Guo, X.; Liu, Y.; Fang, Z.; Zhang, M.; Zhang, R.; You, L.; Li, T.; Liu, R.H. A Full Utilization of Rice Husk to Evaluate Phytochemical Bioactivities and Prepare Cellulose Nanocrystals. *Sci. Rep.* **2018**, *8*, 10482. [CrossRef]
47. Olanipekun, E.A.; Olusola, K.O.; Ata, O. A Comparative Study of Concrete Properties Using Coconut Shell and Palm Kernel Shell as Coarse Aggregates. *Build Environ.* **2006**, *41*, 297–301. [CrossRef]

48. Ranaraja, C.D.; Devasurendra, J.W.; Maduwantha, M.I.P.; Madhuwantha, G.A.L.; Hansa, R.Y.D. Optimization of an Industrial Boiler Operation. *Ournal Res. Technol. Eng.* **2020**, *1*, 126–134.
49. Zhongqing Ma; Jiewang Ye; Chao Zhao; Qisheng Zhang Gasification of Rice Husk in a Downdraft Gasifier: The Effect of Equivalence Ratio on the Gasification Performance, Properties, and Utilization Analysis of Byproducts of Char and Tar. *Bioresources* **2015**, *10*, 2888–2902.
50. Bhatia, B.E.A. *Overview of Refractory Materials*; Meadow Estates Drive Fairfax: Virginia, GA, USA, 2020.
51. Gong, K.; Cao, Y.; Feng, Y.; Liu, S.; Qin, J. Influence of Secondary Reactions on Heat Transfer Process during Pyrolysis of Hydrocarbon Fuel under Supercritical Conditions. *Appl. Therm. Eng.* **2019**, *159*, 113912. [CrossRef]
52. Strezov, V.; Evans, T.J.; Hayman, C. Thermal Conversion of Elephant Grass (Pennisetum Purpureum Schum) to Bio-Gas, Bio-Oil and Charcoal. *Bioresour. Technol.* **2008**, *99*, 8394–8399. [CrossRef] [PubMed]
53. Cheung, K.-Y.; Lee, K.-L.; Lam, K.-L.; Chan, T.-Y.; Lee, C.-W.; Hui, C.-W. Operation Strategy for Multi-Stage Pyrolysis. *J. Anal. Appl. Pyrolysis* **2011**, *91*, 165–182. [CrossRef]
54. Said, M.M.; Mhilu, C.F.; John, G.R. Thermal Characteristics And Kinetics Of Rice Husk For Pyrolysis Process. *Int. J. Renew. Energy Res.* **2014**, *4*, 275–278.
55. Fonts, I.; Azuara, M.; Gea, G.; Murillo, M.B. Study of the Pyrolysis Liquids Obtained from Different Sewage Sludge. *J. Anal. Appl. Pyrolysis* **2009**, *85*, 184–191. [CrossRef]
56. Domínguez, A.; Menéndez, J.A.; Inguanzo, M.; Pís, J.J. Production of Bio-Fuels by High Temperature Pyrolysis of Sewage Sludge Using Conventional and Microwave Heating. *Bioresour. Technol.* **2006**, *97*, 1185–1193. [CrossRef] [PubMed]
57. ben Hassen Trabelsi, A.; Ghrib, A.; Zaafouri, K.; Friaa, A.; Ouerghi, A.; Naoui, S.; Belayouni, H. Hydrogen-Rich Syngas Production from Gasification and Pyrolysis of Solar Dried Sewage Sludge: Experimental and Modeling Investigations. *Biomed Res. Int.* **2017**, *2017*, 7831470. [CrossRef]
58. Fan, H.; Zhou, H.; Wang, J. Pyrolysis of Municipal Sewage Sludges in a Slowly Heating and Gas Sweeping Fixed-Bed Reactor. *Energy Convers. Manag.* **2014**, *88*, 1151–1158. [CrossRef]
59. Biomass Gasification—Biomass (Solid Waste/Sludge) Gasification. Available online: https://blog.nus.edu.sg/chbewch/gasification-technology/biomass-gasification/ (accessed on 23 December 2022).
60. Wang, W. A Thermal Conversion Efficiency Study on Biomass Gasification of Arundo Donax and Woodchips. Master's Thesis, Eastern Illinois University, Charleston, IL, USA, 2013.
61. Biomass Gasification Research—HHV of Syn-Gas. Available online: https://www.eiu.edu/energy/hhv_of_syn_gas.pdf (accessed on 23 December 2022).
62. Rahmat, N.F.H.; Rasid, R.A. Gasification of Empty Fruit Bunch with Carbon Dioxide in an Entrained Flow Gasifier for Syngas Production. *IOP Conf. Ser. Mater. Sci. Eng.* **2017**, *206*, 012013. [CrossRef]
63. Sultan, S.H.; Palamanit, A.; Techato, K.-A.; Amin, M.; Baloch, K.A. Physiochemical Characterization and Potential of Synthesis Gas Production from Rubber Wood Biomass by Using Downdraft Gasifier. *Mehran Univ. Res. J. Eng. Technol.* **2021**, *40*, 1–15. [CrossRef]
64. Inguanzo, M.; Domínguez, A.; Menéndez, J.A.; Blanco, C.G.; Pis, J.J. On the Pyrolysis of Sewage Sludge: The Influence of Pyrolysis Conditions on Solid, Liquid and Gas Fractions. *J. Anal. Appl. Pyrolysis* **2002**, *63*, 209–222. [CrossRef]
65. Jindo, K.; Mizumoto, H.; Sawada, Y.; Sanchez-Monedero, M.A.; Sonoki, T. Physical and Chemical Characterization of Biochars Derived from Different Agricultural Residues. *Biogeosciences* **2014**, *11*, 6613–6621. [CrossRef]
66. Nguyen, B.T.; Lehmann, J. Black Carbon Decomposition under Varying Water Regimes. *Org. Geochem.* **2009**, *40*, 846–853. [CrossRef]
67. Harvey, O.R.; Herbert, B.E.; Kuo, L.-J.; Louchouarn, P. Generalized Two-Dimensional Perturbation Correlation Infrared Spectroscopy Reveals Mechanisms for the Development of Surface Charge and Recalcitrance in Plant-Derived Biochars. *Environ. Sci. Technol.* **2012**, *46*, 10641–10650. [CrossRef]
68. Harvey, O.R.; Kuo, L.-J.; Zimmerman, A.R.; Louchouarn, P.; Amonette, J.E.; Herbert, B.E. An Index-Based Approach to Assessing Recalcitrance and Soil Carbon Sequestration Potential of Engineered Black Carbons (Biochars). *Environ. Sci. Technol.* **2012**, *46*, 1415–1421. [CrossRef] [PubMed]
69. Rutherford, D.W.; Wershaw, R.L.; Rostad, C.E.; Kelly, C.N. Effect of Formation Conditions on Biochars: Compositional and Structural Properties of Cellulose, Lignin, and Pine Biochars. *Biomass Bioenergy* **2012**, *46*, 693–701. [CrossRef]
70. Spokas, K.A. Review of the Stability of Biochar in Soils: Predictability of O:C Molar Ratios. *Carbon Manag.* **2010**, *1*, 289–303. [CrossRef]
71. Wu, W.; Yang, M.; Feng, Q.; McGrouther, K.; Wang, H.; Lu, H.; Chen, Y. Chemical Characterization of Rice Straw-Derived Biochar for Soil Amendment. *Biomass Bioenergy* **2012**, *47*, 268–276. [CrossRef]
72. Dong, X.; Ma, L.Q.; Zhu, Y.; Li, Y.; Gu, B. Mechanistic Investigation of Mercury Sorption by Brazilian Pepper Biochars of Different Pyrolytic Temperatures Based on X-Ray Photoelectron Spectroscopy and Flow Calorimetry. *Environ. Sci. Technol.* **2013**, *47*, 12156–12164. [CrossRef]
73. Yang, H.; Yan, R.; Chen, H.; Lee, D.H.; Zheng, C. Characteristics of Hemicellulose, Cellulose and Lignin Pyrolysis. *Fuel* **2007**, *86*, 1781–1788. [CrossRef]
74. Khodadad, C.L.M.; Zimmerman, A.R.; Green, S.J.; Uthandi, S.; Foster, J.S. Taxa-Specific Changes in Soil Microbial Community Composition Induced by Pyrogenic Carbon Amendments. *Soil. Biol. Biochem.* **2011**, *43*, 385–392. [CrossRef]

75. Guo, J.; Chen, B. Insights on the Molecular Mechanism for the Recalcitrance of Biochars: Interactive Effects of Carbon and Silicon Components. *Environ. Sci. Technol.* **2014**, *48*, 9103–9112. [CrossRef] [PubMed]
76. Mimmo, T.; Panzacchi, P.; Baratieri, M.; Davies, C.A.; Tonon, G. Effect of Pyrolysis Temperature on Miscanthus (Miscanthus × Giganteus) Biochar Physical, Chemical and Functional Properties. *Biomass Bioenergy* **2014**, *62*, 149–157. [CrossRef]
77. Kalderis, D.; Kotti, M.S.; Méndez, A.; Gascó, G. Characterization of Hydrochars Produced by Hydrothermal Carbonization of Rice Husk. *Solid Earth* **2014**, *5*, 477–483. [CrossRef]
78. Illankoon, W.A.M.A.N.; Milanese, C.; Girella, A.; Medina-Llamas, M.; Magnani, G.; Pontiroli, D.; Ricco, M.; Collivignarelli, M.C. Sabrina Sorlini Biochar derived from the rice industry by-products as sustainable energy storage material. In *Proceedings of the 30th European Biomass Conference and Exhibition (EUBCE), Online, 9–12 May 2022*; Chevet, P.-F., Scarlat, N., Grassi, A., Eds.; ETA-Florence Renewable Energies: Florence, Italy, 2022.
79. Weber, K.; Quicker, P. Properties of Biochar. *Fuel* **2018**, *217*, 240–261. [CrossRef]
80. Lee, J.W.; Kidder, M.; Evans, B.R.; Paik, S.; Buchanan, A.C., III; Garten, C.T.; Brown, R.C. Characterization of Biochars Produced from Cornstovers for Soil Amendment. *Environ. Sci. Technol.* **2010**, *44*, 7970–7974. [CrossRef]
81. Yuan, J.-H.; Xu, R.-K.; Zhang, H. The Forms of Alkalis in the Biochar Produced from Crop Residues at Different Temperatures. *Bioresour. Technol.* **2011**, *102*, 3488–3497. [CrossRef] [PubMed]
82. Parr, J.F. Effect of Fire on Phytolith Coloration. *Geoarchaeology* **2006**, *21*, 171–185. [CrossRef]
83. Wilding, L.P.; Brown, R.E.; Holowaychuk, N. Accessibility and Properties of occluded carbon in biogenetic opal. *Soil Sci.* **1967**, *103*, 56–61. [CrossRef]
84. Gong, J.; Li, J.; Xu, J.; Xiang, Z.; Mo, L. Research on Cellulose Nanocrystals Produced from Cellulose Sources with Various Polymorphs. *RSC Adv.* **2017**, *7*, 33486–33493. [CrossRef]